Controlling Lane-Free Signal-Free Intersections via Model Predictive Control

Mehdi Naderi*[1], Panagiotis Typaldos [1], Markos Papageorgiou [1,2]

[1] Dynamic Systems and Simulation Lab, Technical University of Crete, Greece

[2] Faculty of Maritime and Transportation, Ningbo University, Ningbo, China

SHORT SUMMARY

The operation of signal-free intersections, where connected automated vehicles (CAVs) cross simultaneously for all origin-destination (OD) movements, has the potential to greatly increase throughput and decrease fuel consumption. Since the intersection crossing areas naturally include no lanes, an extended crossing area, appropriately delineated, can be considered as a lane-free infrastructure so as to enable further improved exploitation. This paper presents a Model Predictive Control (MPC) scheme to manage CAVs on a signal-free and lane-free intersection. In fact, the control inputs of all vehicles are optimized over a time-horizon by online solving of a joint optimal control problem (OCP) that minimizes a cost function including proper terms to ensure smooth and collision-free vehicle motion, while also considering fuel consumption and desired-speed tracking, when possible. An efficient and fast Feasible Direction Algorithm is employed to solve the introduced OCP numerically. Simulation results verify the effectiveness of the presented approach and its computational feasibility as a real-time scheme.

Keywords: Automated and connected driving, Lane-free traffic, Model Predictive Control, Optimal Control, Signal-free intersection.

1. INTRODUCTION

The TrafficFluid concept, a novel paradigm for vehicular traffic, applicable at high levels of vehicle automation, was recently proposed by Papageorgiou et al. (2021) and relies on two combined principles: (a) Lane-free traffic, whereby vehicles are not forced to move on fixed traffic lanes, but may drive anywhere on the 2-D surface of the road; and (b) Vehicle nudging, whereby vehicles may influence the movement of other vehicles not only behind, but also on the sides or in front of them. By its nature, the crossing area of urban intersections has no fixed lanes and may therefore be considered as lane-free network elements.

While many existing works focus on the development of signal-free intersections, see for instance (Zhong et al. 2020, Niels et al. 2023), lane-free intersection operation is a relatively new concept addressed in a few works which let vehicles drive on any position of the intersection's 2-D crossing area surface, instead of following fixed pre-defined paths, as proposed in lane-based intersection control strategies. In a sequence of papers, Li et al. (2018; 2020; 2021; 2023) formulate a joint (all vehicles) constrained optimal control problem (OCP) to maximize vehicle advancement and hence intersection throughput but have to apply various significant simplifications to mitigate very high computational requirements for the numerical solution. For example, Li et al. (2023) suggest an online strategy that introduces small disjoint vehicle 'batches' crossing the intersection one at a time, for each of which a small-scale OCP is considered, while the batch crossing order is determined by a FIFO policy. Another lame-free joint optimal control approach is proposed by Amouzadi et al. (2022a, 2022b), minimizing the final time, at which all vehicles arrive at their pre-selected final positions; while considering physical limits and avoiding collisions by defining

appropriate constraints. Furthermore, Ahmadi and Carlson (2023) present a centralized MPC strategy to advance towards their destinations, while minimizing their distance from a pre-defined reference path and the energy consumption. These approaches mainly suffer from high computational burden that may prevent online implementation in presence of many vehicles.
In (Naderi et. al 2024), we have recently proposed a joint OCP for vehicles crossing a signal-free and lane-free intersection that does not include limiting assumptions, like specific initial and final conditions which may reduce the solution flexibility. The cost function includes proper terms to reflect control input magnitude, deviation from desired speed and desired orientation, and collision avoidance; and leads to safe, smooth, and efficient vehicle movements. Appropriate constraints are introduced for physical limits and boundary respect. The formulated constrained OCP was solved offline by an efficient Feasible Direction Algorithm (FDA) which is very fast and real-time feasible.

In this work, we use the OCP by (Naderi et. al 2024) to develop a model predictive control (MPC) strategy that determines in real-time the optimal control trajectory of vehicles crossing a signal-free intersection in lane-free mode. The proposed MPC procedure is preliminarily tested and demonstrated via a realistic scenario and corresponding video.

2. VEHICLE DYNAMICS AND INPUT CONSTRAINTS

This section describes the vehicle model, along with the state-dependent control constraints.

Vehicle Dynamics

Due to frequent and strong turnings while crossing the intersection, a relatively accurate model like the kinematic bicycle model should be employed to represent the vehicle dynamics, as described by the following state equations (Karafyllis et al. 2022):

$$\begin{aligned} \dot{x} &= v\cos(\theta) \\ \dot{y} &= v\sin(\theta) \\ \dot{\theta} &= \sigma^{-1} v\tan(\delta) \\ \dot{v} &= F \end{aligned} \tag{1}$$

where x and y are the longitudinal and lateral position coordinates of the vehicle's rear axle midpoint; v is the vehicle speed; θ is its orientation; and σ is the vehicle length. Acceleration F and steering angle δ are control inputs. For practical uses, such as simulator or discrete-time OCPs, the bicycle model needs to be discretized. The exact sampled-data model reads (Theodosis et al. 2022):

$$\begin{aligned} x(k+1) &= x(k) + \frac{\sigma}{\tan(\delta(k))} * \left(\sin\left(\theta(k) + v(k)\frac{\tan(\delta(k))}{\sigma} T + F(k)\frac{\tan(\delta(k))}{2\sigma} T^2 \right) - \sin\left(\theta(k)\right) \right) \\ y(k+1) &= y(k) + \frac{\sigma}{\tan(\delta(k))} * \left(\cos\left(\theta(k)\right) - \cos\left(\theta(k) + v(k)\frac{\tan(\delta(k))}{\sigma} T + F(k)\frac{\tan(\delta(k))}{2\sigma} T^2 \right) \right) \\ \theta(k+1) &= \theta(k) + v(k)\frac{\tan(\delta(k))}{\sigma} T + F(k)\frac{\tan(\delta(k))}{2\sigma} T^2 \\ v(k+1) &= v(k) + F(k)T \end{aligned} \tag{2}$$

where T is the sampling period.

Steering Angle Bounds

Two sets of bounds for the steering angle are included in the OCP to account, respectively, for: 1) OD corridor boundary respect; 2) centrifugal acceleration limit.

Firstly, to guarantee that vehicles remain within the intersection boundaries, but also avoid abrupt changes in their movements, and successfully reach their destinations, we establish appropriate overlapping OD (Origin-Destination) corridors (Naderi et. al. 2024), whose boundaries are partly circular and partly straight. Vehicles with specific intentions (straight, left, or right) are allowed to move within the corresponding OD corridor. The designed corridors for straight-going, right-turning, and left-turning vehicles entering from the left arm are shown in Fig. 1. The radii of circular parts are selectable based on which other parameters are calculated, for details see (Naderi et. al. 2024). Note that, for higher flexibility and efficiency, we allow the left-turning corridors to start at a distance L_{start} from the intersection center (see Fig. 1), which creates an extended crossing area.

In order to maintain vehicles within the designated OD corridors, two linear boundary controllers (BCs) have been developed for the left and right boundaries, either circular or straight, delivering upper and lower bounds for the vehicle's steering angle. A BC would asymptotically navigate a vehicle to the corresponding boundary and would then have it driving on the boundary if it remains permanently active. To ensure that the left and right boundaries will not be violated, appropriate boundary controllers are derived in (Naderi et. al. 2024) that are used as lower limit $\underline{\delta}_{\text{B}}(\boldsymbol{x}(k))$ and upper limit $\overline{\delta}_{\text{B}}(\boldsymbol{x}(k))$ for the steering angle.

Secondly, to provide passenger comfort, we limit the steering angle such that the centrifugal acceleration does not exceed a comfort threshold. To this end, $|\delta(k)| \le \tan^{-1}(\sigma F_{\text{c,max}} / v^2(k))$ should be satisfied, where $F_{\text{c,max}}$ is the comfort limit for the centrifugal acceleration.

To summarize, the state-dependent constraints for steering angle of a vehicle are:

$$\begin{aligned} &\underline{\delta}(\boldsymbol{x}(k)) \le \delta(k) \le \overline{\delta}(\boldsymbol{x}(k)) \\ &\underline{\delta}(\boldsymbol{x}(k)) = \max\left(-\tan^{-1}(\sigma F_{\text{c,max}} / v^2(k)), \underline{\delta}_{\text{B}}(\boldsymbol{x}(k))\right) \\ &\overline{\delta}(\boldsymbol{x}(k)) = \min\left(\tan^{-1}(\sigma F_{\text{c,max}} / v^2(k)), \overline{\delta}_{\text{B}}(\boldsymbol{x}(k))\right) \end{aligned} \tag{3}$$

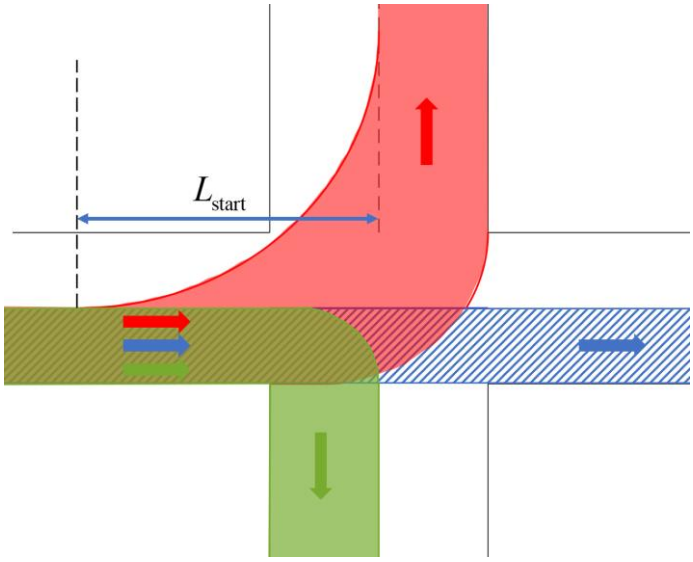

Figure 1: OD corridors

Acceleration Bounds

The first issue to address in terms of acceleration is the practical limits, as each vehicle can generate accelerations from a limited range, i.e. $[F_{\min}, F_{\max}]$. Furthermore, negative or higher-than-maximum ($v_{\max}$) speed values are avoided by defining proper state-dependent lower and upper bounds for the acceleration that are derived from the state equation of speed. In conclusion, acceleration constraints are constructed as:

$$\begin{aligned} &\underline{F}(\boldsymbol{x}(k)) \le F(k) \le \bar{F}(\boldsymbol{x}(k)) \\ &\underline{F}(\boldsymbol{x}(k)) = \max(F_{\min}, -v(k)/T) \\ &\bar{F}(\boldsymbol{x}(k)) = \min(F_{\max}, (v_{\max} - v(k))/T) \end{aligned} \tag{4}$$

Note that in (3) and (4) smoothified max and min-functions are used. Also, we transform the state-dependent constraints to constant control input bounds by replacing the control inputs as below:

$$\begin{aligned} F_i(k) &= (1-u_{F,i}(k))\underline{F}_i(\boldsymbol{x}(k)) + u_{F,i}(k)\bar{F}_i(\boldsymbol{x}(k)) \\ \delta_i(k) &= (1-u_{\delta,i}(k))\underline{\delta}_i(\boldsymbol{x}(k)) + u_{\delta,i}(k)\bar{\delta}_i(\boldsymbol{x}(k)) \end{aligned} \tag{5}$$

where $u_{F,i}$ and $u_{\delta,i}$ are new control inputs of vehicle *i* whose values must be in the range of $[0,1]$.

3. THE OPTIMAL CONTROL PROBLEM

In this section, a joint optimal control problem is formulated, minimizing a weighted sum of multiple sub-objectives for all considered vehicles to provide safe, smooth, and efficient intersection crossing. The objective function and numerical solution algorithm are presented. Finally, an MPC scheme is described.

Objective Function

The introduced objective function for each vehicle i includes a few weighted terms, each of which reflects a specific goal, as explained below.

1) Fuel consumption and passenger comfort

As shown by Typaldos et al. (2020), minimizing the square-of-acceleration leads to fuel-minimizing vehicle trajectories in OCPs. Therefore, quadratic acceleration $F_i^2(k)$ and steering angle $\delta_i^2(k)$ are included in the cost function that also account for passenger comfort.

2) Desired speed tracking

While crossing the intersection, accurately tracking the desired speed is not the most important goal; however, penalizing deviations from the desired speed $v_{\mathrm{d},i}$ by including $(v_i(k) - v_{\mathrm{d},i})^2$ in the objective function motivates vehicles to advance faste and consequently influences the intersection throughput.

3) Desired orientation tracking

As detailed in (Naderi et al. 2024), we guide vehicles toward their destination branch by defining appropriate desired orientations on any location of the corresponding OD corridor. A vehicle starting at some initial position and driving according to the desired orientations would drive on an ideal path; however, vehicles may deviate from the ideal path due to other important tasks, like

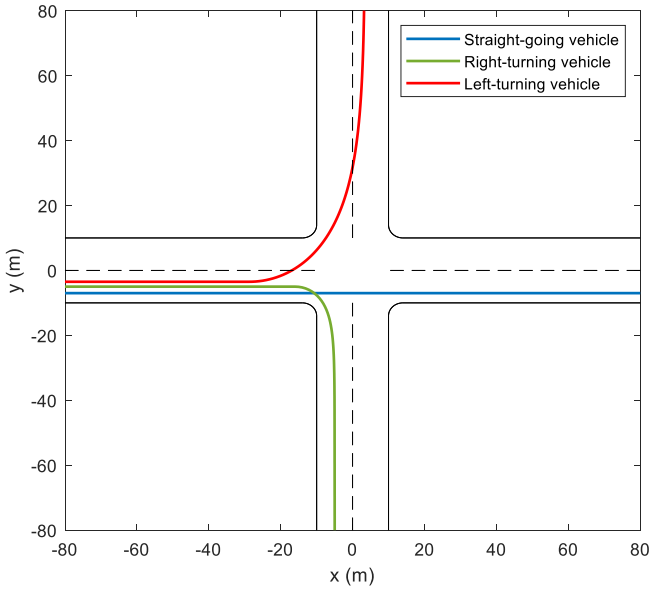

Figure 2: Ideal paths for vehicles

collision avoidance. The desired orientation for turning vehicles gradually changes from the entrance branch to the exit branch orientation, while for the straight-going ones, it remains constant. Fig. 2 illustrates the ideal paths for three typical vehicles with different intentions. Note that the path shape may slightly vary depending on the initial lateral position of the vehicle. Including a term in the objective function that penalizes deviation from the desired orientation, i.e. $(\theta_i(k)-\theta_{\mathrm{d},i}(\boldsymbol{x}(k)))^2$, where $\theta_{\mathrm{d},i}(\boldsymbol{x}(k))$ is the position-dependent desired orientation, encourages vehicles to drive close to the ideal path, whenever possible.

4) Collision avoidance

Given the major conflicts among vehicles with antagonistic ODs, avoiding collisions is of highest importance. This goal may be met by adding the following term for each pair of vehicles i , j to the cost function:

$$c_{i,j}(k) = \gamma_1 \exp\left(-d_{i,j}(k) / \gamma_2\right) \tag{6}$$

where $d_{i,j}(k)$ is the elliptic distance based on the direction of vehicle *i* (see (Naderi et al. 2024)), γ_1 and γ_2 are constant parameters tuning the extent and magnitude of the surrounding 'aura'. As $c_{i,j}(k)$ and $c_{j,i}(k)$ are not equal when two vehicles have different orientations, both terms must be included in the cost function.

5) Deviation of control inputs from the last applied values

Each finite-time control trajectory can start with any feasible value, which, however, may significantly differ from the last applied value, generated by either a previously solved OCP or the branch controller, which may cause passenger discomfort. This can be mitigated by including $(F_i(0)-F_{\mathrm{prev},i})^2$ and $(\delta_i(0)-\delta_{\mathrm{prev},i})^2$ in the cost function, where $F_{\mathrm{prev},i}$ and $\delta_{\mathrm{prev},i}$ are the last applied control inputs.

Based on the aforementioned sub-objectives, the cost function is described as:

$$J=\sum_{k=0}^{K-1}[\sum_{i=1}^{n}\{\omega_1 F_i^2(k)+\omega_2\delta_i^2(k)+\omega_3(v_i(k)-v_{d,i})^2+\omega_4(\theta_i(k)-\theta_{\mathrm{d},i}(\boldsymbol{x}(k)))^2+\omega_5\sum_{\substack{j=1\\ j\neq i}}^{n}c_{i,j}(k)\}]$$
$$+\sum_{i=1}^{n}\{\omega_6(F_i(0)-F_{\mathrm{prev},i})^2+\omega_7(\delta_i(0)-\delta_{\mathrm{prev},i})^2\} \quad (7)$$

where K is the fixed time horizon, n is the number of crossing vehicles, and ω_i, $i=1,2,...,7$, are the positive weights determining the relative importance of the terms. Vehicles are not constrained by fixed final states, potentially leading to improved intersection performance as they can advance without the need to maneuver or decelerate in order to match predefined positions or speeds.

Problem Formulation and Numerical Solution

The introduced optimal control problem can be summarized as:

$$\begin{aligned}&\text{Minimize } J=\sum_{k=0}^{K-1}\Phi[\boldsymbol{x}(k),\boldsymbol{u}(k)]\\ &\boldsymbol{x}(k+1)=\boldsymbol{f}[\boldsymbol{x}(k),\boldsymbol{u}(k)]\\ &\boldsymbol{0}\le\boldsymbol{u}(k)\le\boldsymbol{1}\end{aligned} \quad (8)$$

where $\boldsymbol{x}$ and $\boldsymbol{u}$ include state variables and transformed control inputs of all crossing vehicles, respectively. The formulated joint OCP is solved numerically by use of an efficient Feasible Direction Algorithm (FDA), that exploits the state equation structure and maps the OCP into a Nonlinear Programming problem in the reduced space of control variables, i.e. in a mK-dimensional space, where m is the number of inputs. FDA is an iterative algorithm starting with a given feasible control trajectory. Each iteration attempts to improve the control trajectories, in this work using resilient backpropagation (RPROP), by calculating an appropriate step in the mK-dimensional control space. Finally, the algorithm converges to a local minimum of the cost function. For more details, see (Kotsialos and Papageorgiou, 2004).

Model Predictive Control (MPC) Implementation

An MPC scheme is developed to properly navigate vehicles, which are continuously approaching from different branches, to cross in lane-free mode the signal-free intersection in real-time. The general concept is to repeatedly solve the OCP, every K_{opt} samples, each time for all the vehicles that are currently crossing the intersection or are sufficiently close to the crossing area. More precisely, let us first define (see also Fig. 3):

- The Extended Crossing Area (ECA), which consists of the crossing area plus the adjacent part of the roads up to the distance L_{start}, where left-turning (if any) begins (recall Fig. 1). Thus, the ECA includes all locations where vehicles arriving from different branches may face crossing conflicts.
- The Optimal Control Zone (OCZ), which includes ECA, but extends further upstream on the entering branches, up to a distance L_{opt} from the intersection center.

Within the MPC scheme, the OCP is solved in real-time repeatedly, every K_{opt} samples, and determines the optimal trajectories for all vehicles currently located within the OCZ, over the time horizon K, which is selected long enough to avoid myopic actions. Ideally, the time horizon should allow for all included vehicles to exit. Since $K_{\mathrm{opt}}<K$, the optimal trajectories of a vehicle may be updated several times before the vehicle finally exits. To properly manage the crossing

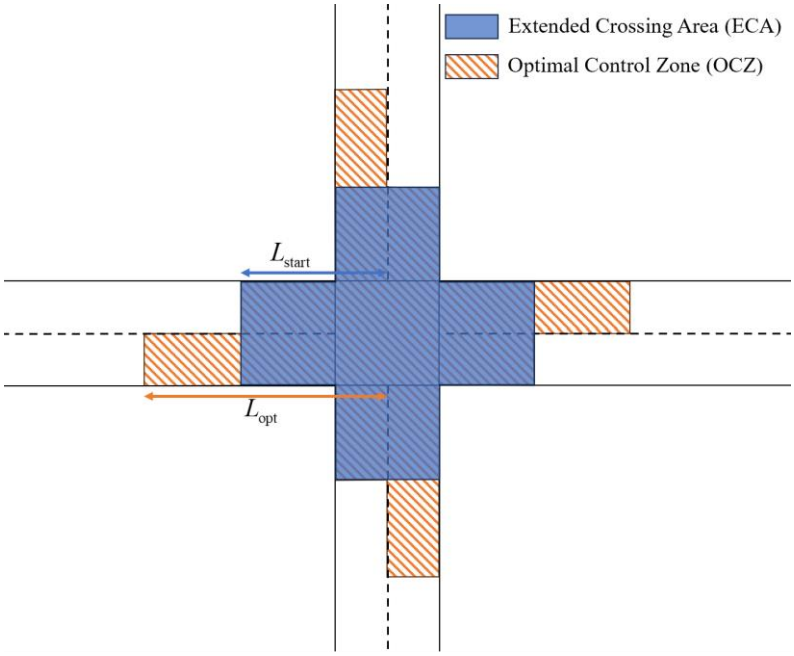

Figure 3: Optimal Control Zone (OCZ) and Extended Crossing Area (ECA)

conflicts, all vehicles located in ECA must always be driving according to the latest run of OCP. But since the OCP is solved every K_{opt} samples, this requirement yields a relationship between L_{opt} and K_{opt}, because a vehicle, which is upstream of OCZ when the last OCP is triggered, and drives with the maximum admissible speed, v_{max}, should not enter ECA in less than $K_{opt}T$ seconds, plus the computation time T_{comp} for solving the OCP. Hence, we get:

$$L_{opt} = L_{start} + v_{max}(K_{opt}T + T_{comp}). \tag{9}$$

After solving the OCP, the first K_{opt} samples of the optimal trajectories are applied to the vehicles which were within OCZ, and a new OCP solution is triggered K_{opt} samples later, and so forth. In the next run of OCP, for vehicles which were previously optimized and are still in OCZ, the rest of their previous optimal control trajectories is considered as the first $K - K_{opt}$ samples of initial guess for the FDA, as this may reduce the number of needed iterations to reach the optimal solution. Finally, vehicles not handled by the OCP are controlled with a nonlinear feedback controller developed in (Karafyllis et al. 2022).

4. RESULTS AND DISCUSSION

To investigate the effectiveness of the proposed MPC scheme, a simulation with vehicles gradually approaching a lane-free signal-free intersection is conducted. The length and width of the considered intersection is 20 m, i.e., the width of each entrance and exit branch is 10 m. All 12 possible Origin Destination (OD) movements are considered. All straight-going flows on the four entering branches are equal, and all right-turning or left-turning rates equal 0.25, which creates an overly challenging crossing scenario. The sampling period is 0.2 s, the optimization horizon is 10 s, and the optimization process is run every 2 seconds (10 samples). Also, the cost function weights are $\omega = [0.005, 1.5, 0.03, 5, 25, 0.1, 1]$. Desired speed is 8 m/s, 10 m/s, and 12 m/s for right-

turning, left-turning, and straight-going vehicles, respectively, and the maximum speed $v_{\max}$ is 15 m/s. In addition, $L_{\text{start}} = 30$ m, $L_{\text{opt}} = 63$ m, $F_{\min} = -3$ m/s^2, $F_{\max} = 1.5$ m/s^2, $F_{\text{c,max}} = 5$ m/s^2, $p = 5$, $\gamma_1 = 1$, $\gamma_2 = 4.5$, and $\sigma = 4.5$ m. The simulation is run in TrafficFluid-Sim (Troullinos et al. 2022) on a machine with an Intel(R) CoreTMi5-10500 CPU @ 3.10GHz with 8.0 GB of installed RAM.

A recorded video of the simulation can be watched at https://bit.ly/3Spm4UU, where vehicles, continuously approaching the intersection, are smoothly and safely guided towards their destinations without exceeding the boundaries. Left-turning vehicles may temporarily use the reverse direction of the roads, which leads to smoother movements and better exploitation of the intersection area.

The number of vehicles included in the OCP may be different every time, and consequently the execution time may vary. Fig. 4 shows the average CPU time (blue dots) needed to solve OCP versus the number n of OCZ vehicles, with a maximum time of 0.508 s when 16 vehicles are optimized simultaneously. Fitting a quadratic function for the CPU time (red curve in Fig. 4), yields $0.0014n^2 + 0.0103n - 0.0068$, which is highly promising for real-time implementation even for bigger intersections.

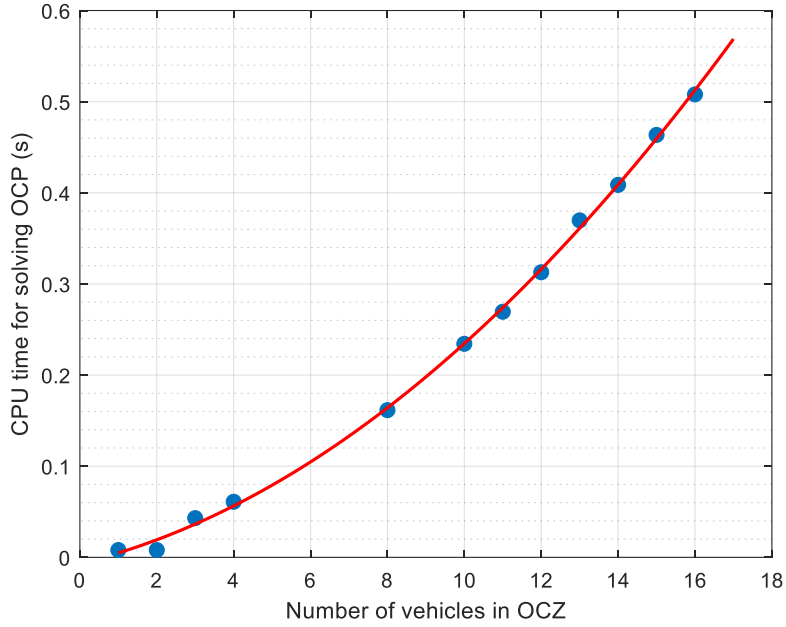

Figure 4: Average CPU time versus included vehicles in OCP

5. CONCLUSIONS

In this paper, a centralized MPC strategy is proposed to control automated vehicles crossing lane-free signal-free intersections. First, a joint optimal control problem is formulated whose cost function includes appropriate terms to facilitate smooth, collision-free, and comfortable movements, while also considering energy consumption and deviation from desired speed. State-dependent constraints are introduced to meet physical limits and keep vehicles within intersection boundaries. Employing FDA, a fast numerical algorithm, the OCP is solved repeatedly to determine the optimal control trajectories for all crossing vehicles. The simulation results confirm that the

suggested MPC strategy leads to suitable vehicle behavior and has the potential to be implemented in a real-time scheme.

ACKNOWLEDGEMENTS

The research leading to these results has received funding from the European Research Council under the European Union's Horizon 2020 Research and Innovation Programme / ERC Grant Agreement no. 833915, project TrafficFluid, see: https://www.trafficfluid.tuc.gr

REFERENCES

Amouzadi M., Orisatoki M.O., Dizqah A.M. 2022a, Lane-free crossing of CAVs through intersections as a minimum-time optimal control problem. *IFAC-PapersOnLine*, Vol. 55, No. 14, pp.28-33.

Amouzadi M., Orisatoki M.O., Dizqah A.M. 2022b, Optimal lane-free crossing of CAVs through intersections , *IEEE Transactions on Vehicular Technology*, Vol. 72, No. 2, pp. 1488-1500.

Ahmadi E., Carlson R.C. 2023, Model predictive control of connected vehicles under automated driving at path-free signal-free intersections, *Transportes*, Vol. 31, No. 3, pp. 1-16.

Karafyllis I., Theodosis D., Papageorgiou M. 2022, Lyapunov-based two-dimensional cruise control of autonomous vehicles on lane-free roads, *Automatica*, Vol. 145, 110517.

Kotsialos A., Papageorgiou M. 2004, Nonlinear optimal control applied to coordinated ramp metering, *IEEE Transactions on Control Systems Technology*, Vol. 12, No. 6, pp. 920-933.

Li B., Zhang Y. 2018, Fault-tolerant cooperative motion planning of connected and automated vehicles at a signal-free and lane-free intersection, *IFAC-PapersOnLine*, Vol. 51, No. 24, pp. 60-67.

Li B., Zhang Y, Jia N., Peng X. 2020, Autonomous intersection management over continuous Space: A microscopic and precise solution via computational optimal control, *IFAC-PapersOnLine*, Vol. 53, No. 2, pp. 17071-17076.

Li B., Zhang Y, Acarman T., Ouyang Y., Yaman C., Wang Y. 2021, Lane-free autonomous intersection management: A batch processing framework integrating reservation-based and planning-based methods, *IEEE International Conference on Robotics and Automation (ICRA)*, pp. 7915-7921.

Li B., Cao D., Tang S., Zhang T., Dong H., Wang Y., Wang F.Y. 2023, Sharing traffic priorities via cyber–physical–social intelligence: A lane-free autonomous intersection management method in metaverse. *IEEE Transactions on Systems, Man, and Cybernetics: Systems*, Vol. 53, No. 4, pp. 2025-2036.

Naderi M., Typaldos P., Papageorgiou M. 2024, Optimal Control of Automated Vehicles Crossing a Lane-free Signal-free Intersection, *European Control Conference (ECC)*, submitted.

Niels T., Bogenberger K., Papageorgiou M., Papamichail I. 2023, Optimization-Based Intersection Control for Connected Automated Vehicles and Pedestrians, *Transportation Research Record*, https://doi.org/10.1177/03611981231172956.

Papageorgiou M., Mountakis K.S., Karafyllis I., Papamichail I., Wang Y. 2021, Lane-free artificial-fluid concept for vehicular traffic, *Proceedings of the IEEE*, Vol.109, pp. 114-121.

Rinaldi M., Viti F., Laskaris G. 2020. How to write a good short paper template. *Journal of writing research papers*, Vol. 1, No. 1, pp. 1-10.

Theodosis D., Tzortzoglou F.N., Karafyllis I., Papamichail I., Papageorgiou M. 2022, Sampled-data controllers for autonomous vehicles on lane-free roads, *30th Mediterranean Conference on Control and Automation (MED)*, Athens, Greece, pp. 103-108.

Troullinos D., Chalkiadakis G., Manolis D., Papamichail I., Papageorgiou M. 2022, "Extending SUMO for lane-free microscopic simulation of connected and automated vehicles", *SUMO Conference Proceedings*, pp. 95-103.

Typaldos P., Papamichail I., Papageorgiou M. 2020, Minimization of fuel consumption for vehicle trajectories, *IEEE Transaction on Intelligent Transportation Systems*, Vol. 21, pp. 1716-1726.

Zhong Z., Nejad M., Lee E.E. 2020, Autonomous and semiautonomous intersection management: A survey, *IEEE Intelligent Transportation Systems Magazine*, Vol. 13, No. 2, pp. 53-70.